Chapter 13
Removing Unwanted Noise from Operational Modal Analysis Data

William K. Bonness and David M. Jenkins

Abstract Operational modal analysis data includes the measurement of dynamic signals such as structural vibration data and the corresponding excitation force or pressure. In addition to the desired information, measured structural vibration data can include unwanted electrical noise and vibration energy from adjacent structures. Measured dynamic pressures can contain unwanted signals such as acoustic and vibration induced pressures. In this paper, a noise removal technique is presented in which an unlimited number of unwanted correlated signals can be removed from a set of measured data. In its simplest form, this technique is related to coherent output power (COP). However, unlike COP noise removal, multiple signals can be removed from measured data while retaining the magnitude and phase of the original data required for modal analysis processing. This technique is demonstrated using vibration data and dynamic wall pressure measurements from a thin-walled aluminum cylinder filled with water flowing at 20 ft/s.

Keywords Operational • Modal • Noise • Removal • Processing

13.1 Introduction

Operational modal analysis involves measuring the vibration of a system during operation either because the desired operational excitation is not appropriately represented by traditional impulsive modal impact testing or because the system cannot be conveniently taken off-line. Transfer function data between vibration and input force are traditionally measured and used as input for an experimental modal analysis. However, when the input force cannot be measured, cross-spectrum measurements between accelerometers can be used in place of the transfer function data. Resonance frequency, damping, and operational modes shapes can all be obtained from cross-spectrum measurements between accelerometers placed at locations required to appropriately resolve the structural mode shapes. Occasionally, measurements of dynamic force or pressure can also be made to help determine modal mass.

Measurements of structural vibration or pressure often include unwanted signals not associated with the signals of interest -especially in an operational setting where other machinery or processes are often running. The unwanted signals may be associated with electrical noise, vibration energy from adjacent structures, vibration induced pressures, and acoustic pressures. While various noise removal techniques are available to "clean up" measured data, a conditioned spectral density technique [1] is presented which can remove multiple signals of unwanted noise from measurements of cross-spectra. This technique can be applied to any dynamic signal measurements which meet necessary criteria.

Lauchle and Daniels [2] employed a related subtraction technique using multiple sensors measured simultaneously to remove noise signals from their measurements of turbulent boundary layer (TBL) wall pressure. Naguib, Gravante, and Wark [3] discuss the advantages of an optimal filtering approach compared to a difference approach. In their work, the optimal filtering provides a better estimate of the noise than the difference approach. The optimal filtering approach yields a frequency domain transfer function which is equivalent to the estimated transfer function from the conditioned spectral density for one sensor of interest and one noise sensor. For offline data analysis, the conditioned spectral density allows one to iteratively remove the effects of several additive noise processes. Additionally, these frequency domain transfer functions can be inverse fast Fourier transformed to obtain a finite impulse response estimate without computing the inverse of a large matrix.

W.K. Bonness (✉) • D.M. Jenkins
Applied Research Laboratory, The Pennsylvania State University, P.O. Box 30, State College, PA 16804, USA
e-mail: wkb3@arl.psu.edu

M. Mains (ed.), *Topics in Modal Analysis, Volume 10*, Conference Proceedings of the Society for Experimental Mechanics Series, DOI 10.1007/978-3-319-15251-6_13

13.2 Approach

13.2.1 Noise Removal Scheme

The single-sided cross spectral density function between two measured signals, $x(t)$ and $y(t)$, is defined as

$$G_{xy}(f) = \frac{2}{T}\overline{X^*(f)Y(f)}. \tag{13.1}$$

where T is the time record length, $X(f)$ and $Y(f)$ are the Fourier Transforms of $x(t)$ and $y(t)$, and the asterisk and overbar denote complex conjugate and ensemble average, respectively. The auto spectrum for a single measured signal $x(t)$ is defined as

$$G_{xx}(f) = \frac{2}{T}\overline{X^*(f)X(f)}, \tag{13.2}$$

and the transfer function, $H_{xy}(f)$, between signals $x(t)$ and $y(t)$ is defined as

$$H_{xy}(f) = \frac{G_{xy}(f)}{G_{xx}(f)}. \tag{13.3}$$

The coherence, $\gamma^2_{xy}(f)$, between $x(t)$ and $y(t)$ is defined as

$$\gamma^2_{xy}(f) = \frac{|G_{xy}(f)|^2}{G_{xx}(f)G_{yy}(f)}, \tag{13.4}$$

and the Coherent Output Power (COP) is defined as

$$COP = \gamma^2_{xy}(f)G_{xx}(f). \tag{13.5}$$

When noise does not exist in a system, it is straightforward to measure the noise-free cross-spectrum between the desired signals $x(t)$ and $y(t)$. However when noise, common to both signals, is added to $x(t)$ and $y(t)$, the desired noise-free cross-spectrum can no longer be measured directly.

Using a three sensor model example illustrated in Fig. 13.1, the noise-free cross-spectrum between signals $x(t)$ and $y(t)$ can be obtained when correlated unwanted noise, represented by a third signal $n(t)$, is added to both signals. The conditioned spectral density technique outlined by Bendat and Persol [1] rejects the portion of the measured $x(t)$ and $y(t)$ signals which

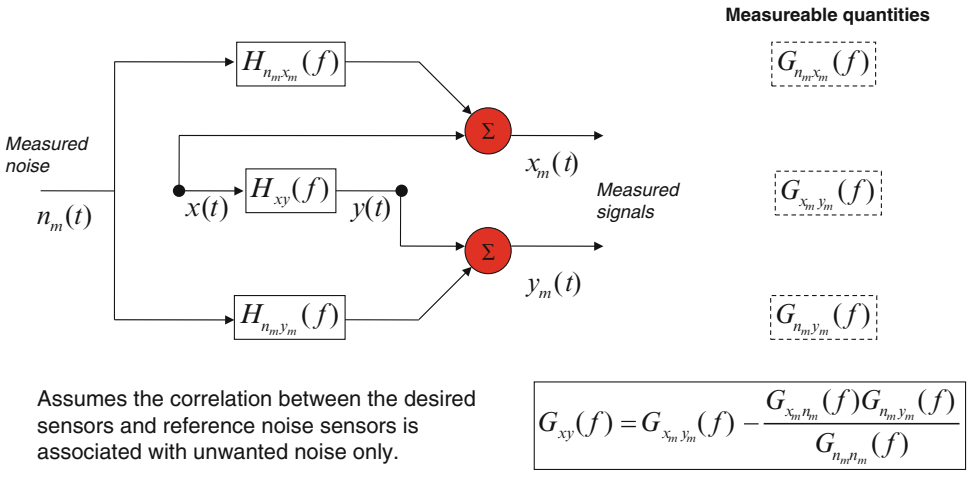

Fig. 13.1 Three sensor model of coherent noise removal process

correlate with the measured noise, $n(t)$. The noise-free cross-spectrum, $G_{xy}(f)$, can be obtained from the measured noisy cross-spectrum, $G_{x_m y_m}(f)$, and spectral measurements involving the noise sensor using

$$G_{xy}(f) = G_{x_m y_m}(f) - \frac{G_{x_m n_m}(f) G_{n_m y_m}(f)}{G_{n_m n_m}(f)}. \tag{13.6}$$

This requires that the cross-spectra between the sensors of interest and reference noise sensor be measured simultaneously. It also assumes that the correlation between the desired sensors and reference noise sensor is associated with unwanted noise only.

For a two sensor model, this noise removal technique reduces to the form,

$$G_{xx}(f) = G_{x_m x_m}(f) - \frac{|G_{x_m n_m}(f)|^2}{G_{n_m n_m}(f)}, \text{ or} \tag{13.7}$$

$$G_{xx}(f) = \left(1 - \gamma^2_{x_m n_m}(f)\right) G_{x_m x_m}(f). \tag{13.8}$$

This form is closely related to the Coherent Output Power (COP) from Eq. (13.5). This form yields a noise free autospectrum, $G_{xx}(f)$, obtained from a noisy autospectrum, $G_{x_m x_m}(f)$, and the coherence, $\gamma^2_{x_m n_m}(f)$, between signal, $x(t)$, and a noise signal, $n(t)$.

This technique can be generalized to include as many reference noise sensors as desired and still retain the cross spectrum between any pair of sensors of interest,

$$G_{xy\cdot(n)!}(f) = G_{xy\cdot(n-1)!}(f) - \frac{G_{xn\cdot(n-1)!}(f) G_{ny\cdot(n-1)!}(f)}{G_{nn\cdot(n-1)!}(f)}, \tag{13.9}$$

where conditioned spectral densities of order n! can be computed from previously known conditioned spectral quantities of order (n−1)!.

To implement this process, one must compute the entire cross-spectral density matrix using all signals including both signals of interest and measured noise signals. It is easiest to implement if the noise signals are at the end of the matrix. One must choose a reference noise signal and remove the correlated portion of this reference signal from all remaining cross-spectra in accordance with Eq. (13.9). This creates a new cross-spectral density matrix and reduces the dimensions by one. Then, one repeats this process for all reference noise signals. The final cross-spectral density matrix includes only signals of interest after removing the correlated portion of all reference noise signals.

13.2.2 Measured Data

The conditioned spectral density noise removal technique is illustrated using data obtained by Bonness, Capone, and Hambric [4]. They measured cylinder vibrations and TBL dynamic wall pressures from a thin-walled 0.15 m diameter aluminum cylinder internally filled with water (pipe-flow) flowing at 6.1 m/s. The gravity-fed test facility (no moving parts) was designed to minimize background vibration and noise from interfering with TBL induced measured quantities. However, because the TBL levels were so low relative to other sources, the measured data still contained a degree of unwanted noise.

A ring array of 12 accelerometers (PCB W532, sens ∼ 100 mV/g) was attached around the shell at a single axial location corresponding to an evenly spaced circumferential grid as shown in Fig. 13.2. Two line arrays of flush mounted wall pressure sensors (PCB-105 M147, sens. ∼50 mV/psi) were installed downstream of the 0.61 m long test-section also shown in Fig. 13.2. One array was aligned with the flow while the second was perpendicular to the flow. In addition to the sensors installed to measure TBL induced vibration and pressure, additional accelerometers and dynamic pressure sensors were installed at various locations to act as reference sensors measuring unwanted noise. Six reference accelerometers were placed on the test-section supports (solid aluminum blocks) to measure the test-section boundary vibrations at both ends in all three coordinate directions. Figure 13.2 shows the location and number of reference sensors used in the signal removal process. Acceleration is shown on the left and wall pressure is shown on the right. In addition, two reference pressure sensors were installed in the same axial plane as the most upstream TBL sensor, and were installed 120° apart (similar to those of Lauchle and Daniels [2]). The separation distance between the reference pressure sensors and the all TBL pressure sensors results in uncorrelated TBL pressures for all frequencies of interest. Two reference accelerometers were placed in the midst of the TBL pressure sensor arrays to measure local pipe vibrations.

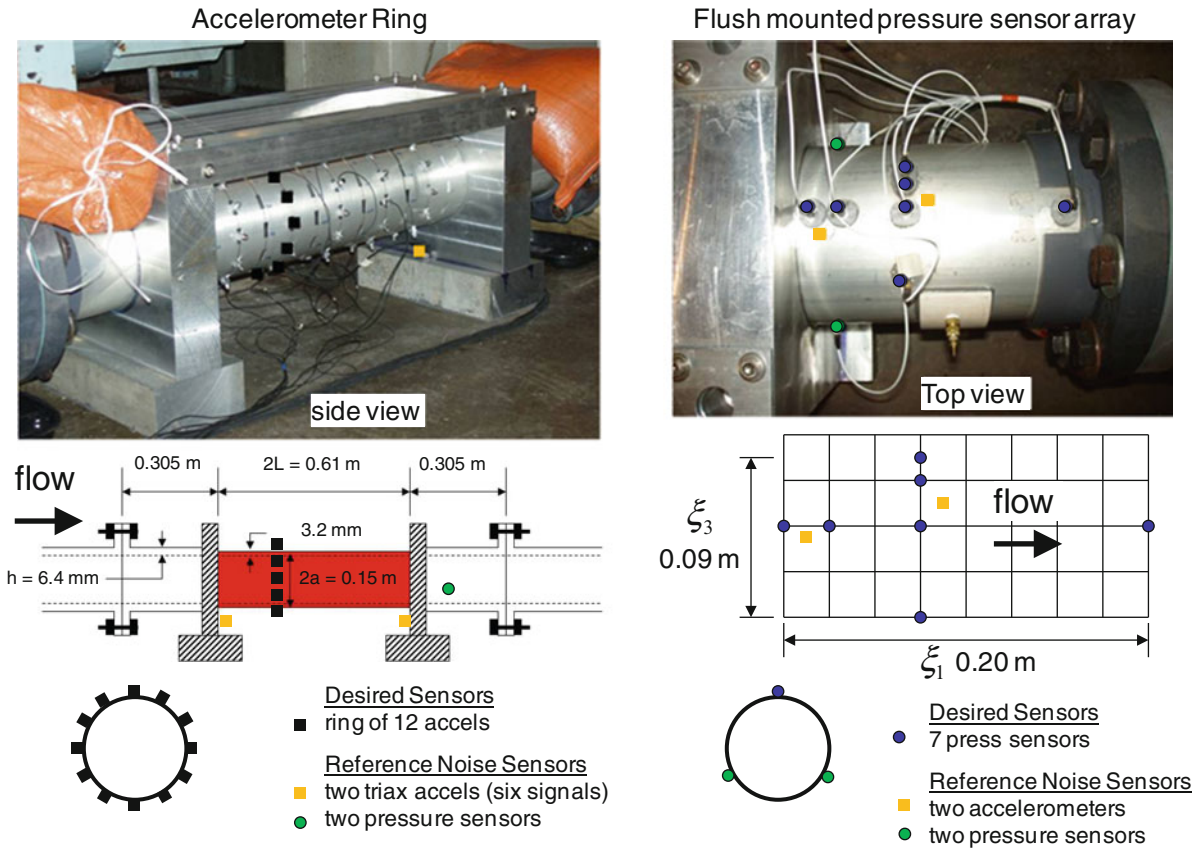

Fig. 13.2 Experimental setup, flow measurement arrays, and reference noise sensor locations

Transfer function data required for the modal analysis can be created from the noise-free cross spectra using an appropriate sensor location (or multiple locations) as the reference location(s) from

$$H_{xy}(f) = \frac{G_{xy}(f)}{|G_{xy}(f)|^{1/2}}. \tag{13.10}$$

13.3 Results

Figure 13.3 shows a spectrogram from a single accelerometer within the circumferential array shown in Fig. 13.2. This plot shows evidence of cylinder vibration before and after flow start and stop and identifies evidence of facility pumps and fans turning on and off during a 4 min data capture period. The 41 s time intervals labeled “less noise” and “more noise” are used in subsequent analyses to demonstrate the noise removal process and results.

It was desirable to remove energy from the measured vibration levels of the 0.61 m long test-section associated with the vibration of adjacent structures. Therefore, accelerometers were placed on the test-section supports in all three coordinate directions and used as reference noise sensors for the circumferential ring of accelerometers. Two pressure sensors were also used as reference noise sensors to remove any acoustic induced vibration. The results of removing the vibration energy correlated with six reference noise accelerometers and two reference pressure sensors are shown in Fig. 13.4. Results for the auto-spectrum of vibration for a single accelerometer are shown on the left side of the figure. The different curves show the progression of results as each reference noise signal was removed in succession. The top curve represents the vibration levels as measured. The bottom curve represents the remaining vibration energy not correlated with any of the eight reference noise sensors. Very little energy in the as-measured vibration spectrum was correlated with the two pressure sensors (p1 and p2), so the resulting spectra after those signals were removed changed very little. Various changes to the vibration spectra occurred

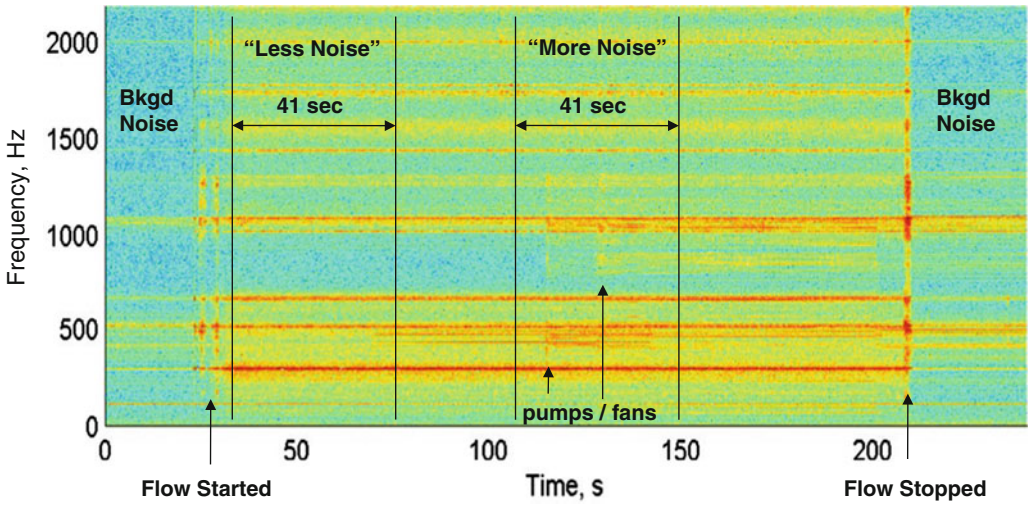

Fig. 13.3 Accelerometer spectrogram showing different levels of extraneous noise in time domain data

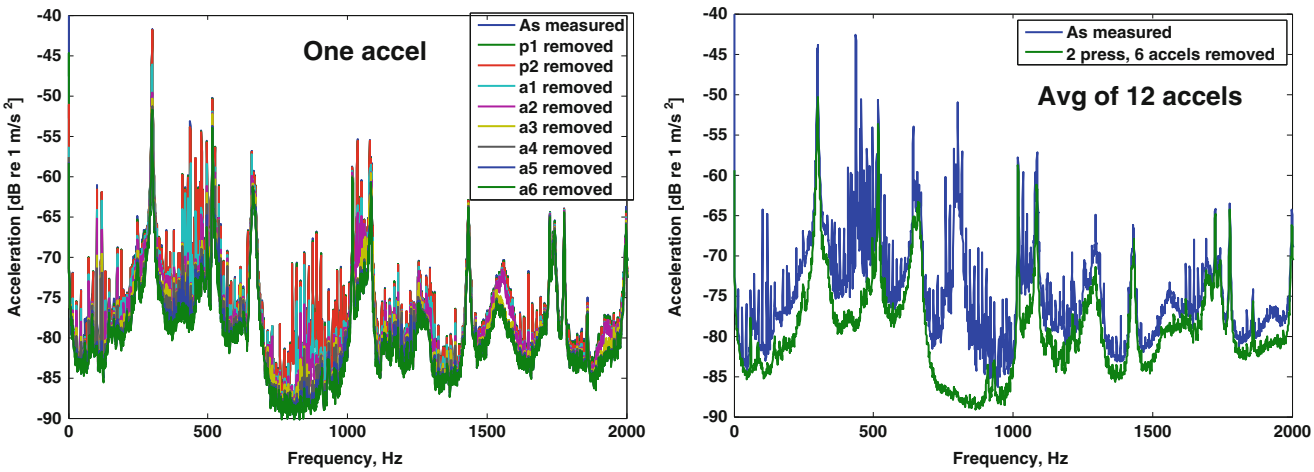

Fig. 13.4 Accelerometer auto-spectra showing progression of noise removal process (*left*) and final before and after noise removal results (*right*)

as each of the six reference accelerometer signals (a1–a6) were removed. Different vibration peaks correlated differently with reference accelerometers oriented in different directions. Some cylinder vibration peaks were reduced by less than 1 dB and some were reduced by as much as 10 dB. The final before and after plot of the noise removal process is shown on the right side of Fig. 13.4 for the average of all 12 accelerometers in the circumferential array.

The different colored curves in the plots shown in Fig. 13.5 represent the circumferential Fourier components of the total measured cylinder vibration spectrum. One must have the cross-spectra between all 12 accelerometers in the circumferential array to determine the individual spatial Fourier components. Figure 13.5 demonstrates the Fourier analysis for two different time segments identified in Fig. 13.3 before and after the conditioned spectral density noise removal technique is applied. For the "more noise" case on the top, a significant difference is evident before and after noise removal. For the "less noise" case on the bottom, very little difference is evident before and after noise removal. The clearly identifiable Fourier components following noise removal indicates that valid cross-spectra was retained. Despite the presence of more or less noise in the originally measured data, the final result is very similar. This provides strong evidence that the noise removal technique works as intended.

In addition to unwanted noise in the accelerometer data, unwanted noise was present in the wall pressure data. Because acoustic pressures and vibration induced pressures produce coherent signals over long distances and the TBL induced wall pressures do not, any portion of a wall pressure sensor signal coherent with a reference noise pressure signal (at a sufficient distance) can be removed leaving only the TBL induced signals. Figure 13.6 shows a progression of results similar to Fig. 13.4 for a wall pressure sensor. Two accelerometers and two pressure sensors were used as reference noise sensors. After applying the noise removal to the as-measured pressure data, the wall pressure levels above 100 Hz were slightly

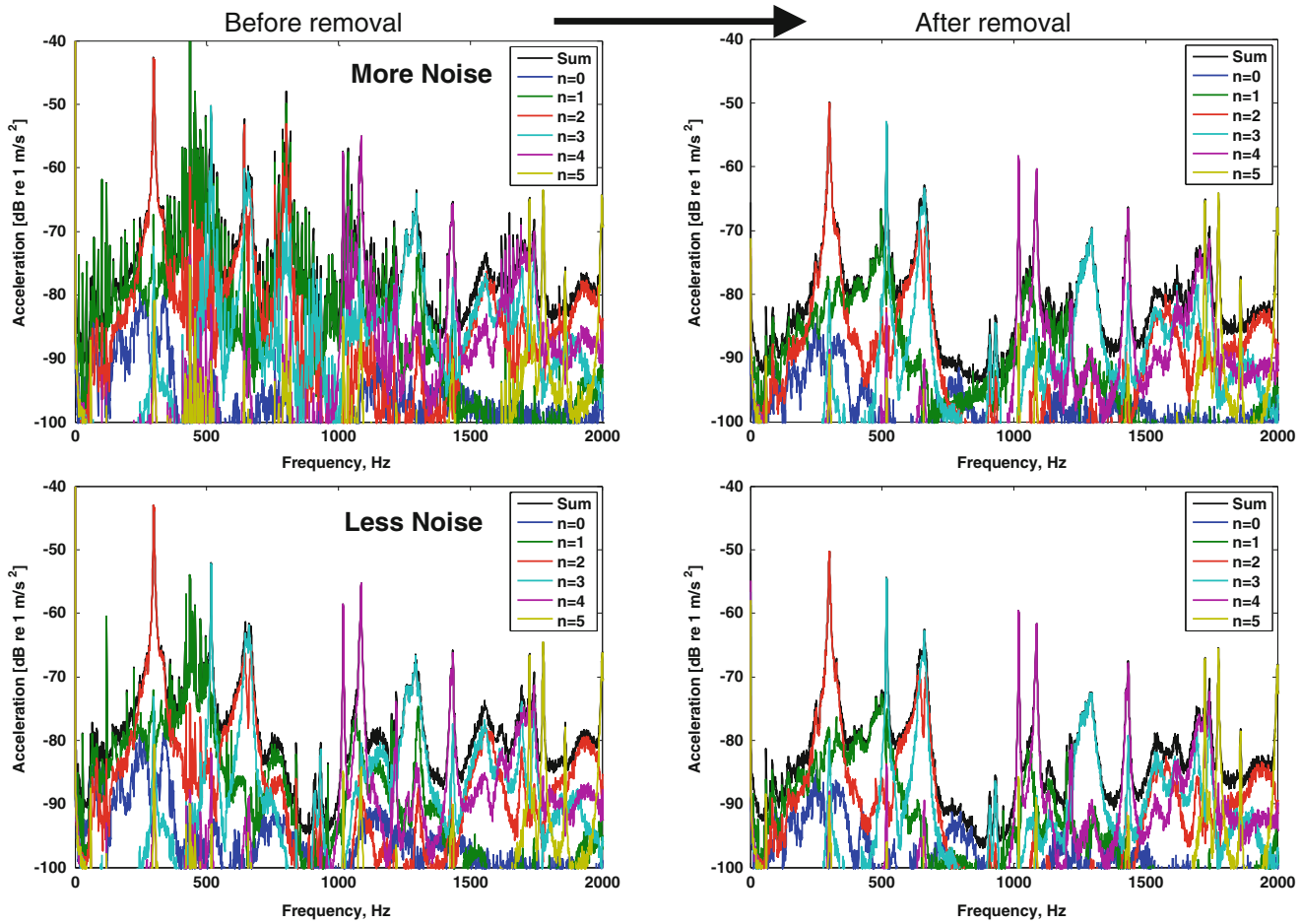

Fig. 13.5 Accelerometer cross-spectra decomposed into circumferential Fourier components. Before and after noise removal results applied to two different time segments identified in Fig. 13.3: noisy data (*top two plots*), less noisy data (*bottom two plots*)

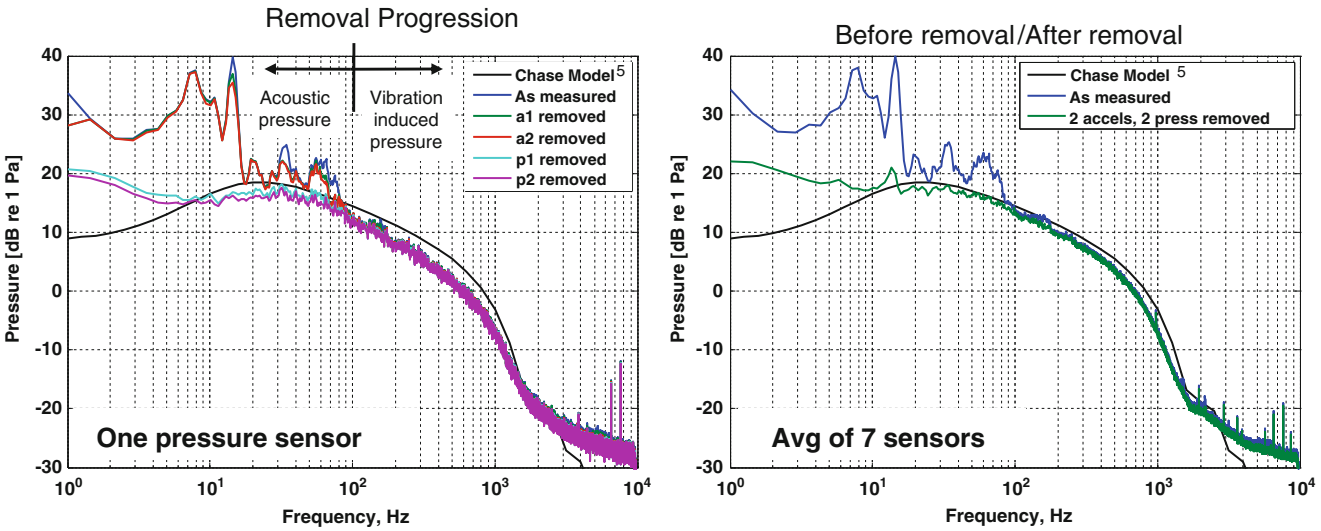

Fig. 13.6 Pressure auto-spectra showing progression of noise removal process (*left*) and final before and after noise removal results (*right*)

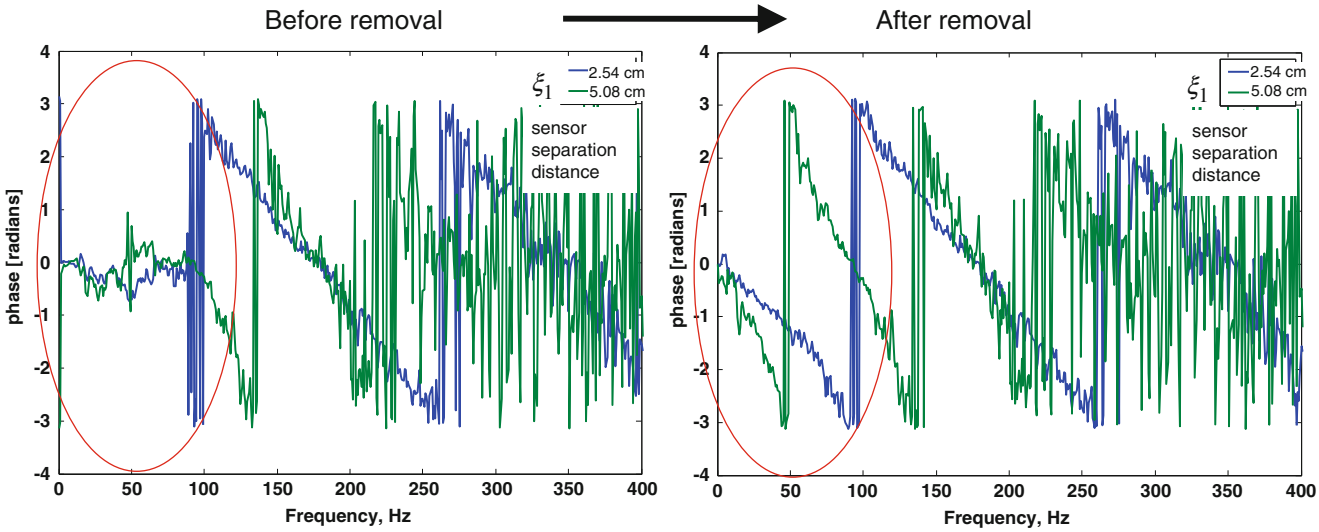

Fig. 13.7 Cross-spectra phase between wall pressure sensors separated in the streamwise direction

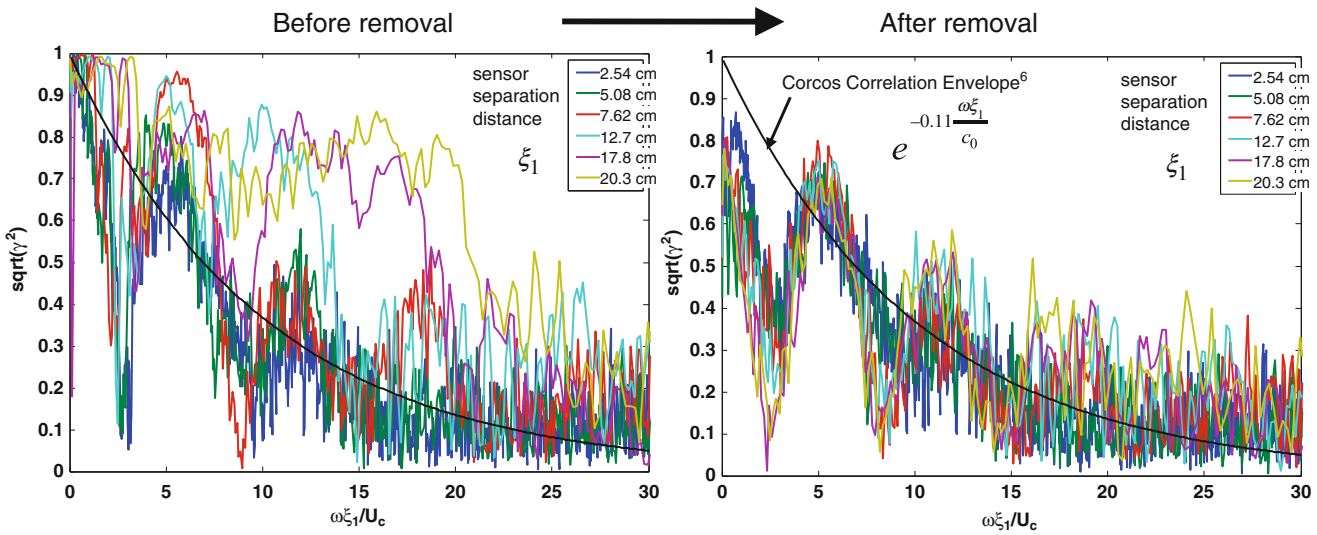

Fig. 13.8 Coherence between wall pressure sensors separated in the streamwise direction

reduced due to correlation between the pressure sensor and the reference accelerometers indicating the presence of vibration induced pressures. Similarly, the wall pressure levels below 100 Hz were significantly reduced due to correlation between the pressure sensor and the reference pressure sensors indicating the presence of acoustic pressures. A theoretical model of the expected TBL wall pressure spectrum from Chase [5] is given as a reference.

Figures 13.7 and 13.8 demonstrate example results using the signal removal technique on measured wall pressure cross-spectra. Figure 13.7 shows the improved phase recovered below 100 Hz between flush mounted TBL pressure sensors in the streamwise direction. Figure 13.8 shows the Corcos [6] correlation function compared with improved coherence recovered between TBL pressure sensors in the streamwise array. Both of these examples provide strong evidence that the noise removal technique works as intended. The full cross-spectra between signals of interest was retained providing improved magnitude and phase.

13.4 Conclusions

Measurements of cross-spectral data between accelerometers can be used in place of traditional transfer function data for an operational modal analysis when the input force cannot be easily measured. Unwanted noise often accompanies these measurements in an operational setting. A noise removal technique based on conditioned spectral densities is presented which allows an unlimited number of unwanted correlated signals to be removed from a set of measured cross-spectra. In its simplest form, this technique is related to the coherent output power and optimal filtering discussed by Naguib et al. [3]. An advantage of this technique over others is that multiple reference noise signals can be removed and the effect of removing each signal can be evaluated. This technique requires measuring reference noise sensors which contain signals that correlate with unwanted noise in the sensors of interest. Reference noise sensors must not contain any signals which correlate with signals of interest in the measured sensors. Measured cylinder vibration and wall pressure cross-spectral data are markedly improved using this noise removal technique. This technique can be applied to any dynamic measurements which meet the necessary criteria.

References

1. Bendat JS, Persol AG (1986) Random data – analysis and measurement procedures. Wiley, New York
2. Lauchle GC, Daniels MA (1987) Wall-pressure fluctuations in turbulent pipe flow. Phys Fluids 30(10):3019–3024
3. Naguib AM, Gravante SP, Wark CE (1996) Extraction of turbulent wall-pressure time-series using an optimal filtering scheme. Exp Fluids 22(1):14–22
4. Bonness WK, Capone DE, Hambric SA (2010) Low-wavenumber turbulent boundary layer wall-pressure measurements from vibration data on a cylinder in pipe flow. J Sound Vib 329(20):4166–4180
5. Chase DM (1987) The character of the turbulent wall pressure spectrum at subconvective wavenumbers and a suggested comprehensive model. J Sound Vib 112:125–147
6. Corcos GM (1964) The structure of the turbulent pressure field in boundary-layer flows. J Fluid Mech 18(3):353–378